Grafting and Phosphonic Acid Functionalization of Hyperbranched Polyamidoamine Polymer onto Ultrafine Silica

Phairat Punyacharoennon, Sireerat Charuchinda, Kawee Srikulkit

Department of Materials Science, Faculty of Science, Chulalongkorn University, Bangkok 10330, Thailand

Received 6 March 2008; accepted 9 June 2008
DOI 10.1002/app.28917
Published online 10 September 2008 in Wiley InterScience (www.interscience.wiley.com).

ABSTRACT: In this study, grafting of hyperbranched polyamidoamine (PAMAM) polymer onto ultrafine silica followed by functionalization via the introduction of phosphonic acid groups into the branch ends was performed. First, an initiating site was incorporated into the silica surface by reacting the silica silanol group with 3-aminopropyltriethoxysilane, producing amino-functionalized silica. The free amine group content was altered by varying the ratio of methanol to water in the hydrolysis step of the silanization reaction. Grafting of PAMAM was attained by three rounds of sequential Michael addition of silica amino groups to methyl acrylate and amidation of the resulting terminal methyl ester groups with ethylenediamine. Completion of the grafting reaction in each step was clearly confirmed using FTIR analysis. Excessive ethylenediamine and unattached hyperbranched PAMAM present in the reaction product were removed by dialysis with a molecular weight cutoff of 6000–7000 Daltons. However, the amino group content determined in each step was found to be significantly lower than theoretically expected, perhaps indicative of side reactions and, in later stages, steric hindrance. The resultant hyperbranched PAMAM-grafted onto silica was functionalized by phosphorylation of the terminal amino groups by a Mannich type reaction, producing the phosphorylated hyperbranched PAMAM-grafted silica. Then its application on cotton fabric to produce fire-retardant cellulose was tentatively investigated. © 2008 Wiley Periodicals, Inc. J Appl Polym Sci 110: 3336–3347, 2008

Key words: hyperbranched PAMAM-grafted silica; phosphorylated hyperbranched PAMAM-grafted silica; phosphonated cellulose; flame retardancy

INTRODUCTION

Polyamidoamine (PAMAM) dendrimers, the starburst polymers with a plurality of terminal functional groups, have recently attracted considerable interest because of their novel functionalities such as nanoscopic containers, delivery devices, ultrafine colloid stabilizers, and nanocomposite materials.[1–8] Surface modifications of terminal groups with different functionalities, such as acetamide, hydroxyl, carboxyl, or quaternized PAMAM dendrimers, have further increased the versatile applicability of these materials.[9–13] In the cases of carbon black and silica nanoparticles, which are promising fillers used in rubber and plastics, a good uniform dispersion of these extremely fine particles within the polymer matrix is important. However, these nanoparticles tend to form micron-sized aggregates with a resulting inferior performance when compared with those of the nanometer-sized form. This problem of a strong tendency for nanoparticles to agglomerate is solved by surface modification, especially incorporation of repulsive-like charges.[14–17] The grafting of PAMAM polymer onto the inorganic particle's surface is one such possibility to effectively prevent agglomerate formation and results in the stability of ultrafine nanoparticles in the colloidal state or a high dispersibility within the polymer matrix.[18–20] Nanometer-sized particle fillers are expected to exhibit attractive interactions with the polymer matrix at very low filler content, resulting in an improved performance of nanocomposite materials. For example, nanomaterials can alter gas permeability, increase solvent resistance, and reduce flammability. Another interesting effect is that PAMAM attachment onto inorganic particles leads to hybrid materials with special characteristics such as high-performance chelating agents[21] and nanoreactors in which the metal nanoparticles are stabilized.[22] In this study, phosphorylated PAMAM-based silica nanoparticles were synthesized in an attempt to impart a significant flame-retardant performance on cotton cellulose. When considering flame retardants for cellulose and cellulose derivatives, phosphorus-based flame compounds have been of major interest because of their relatively environmentally friendly product status, their low toxicity, and their low evolution of smoke

Correspondence to: K. Srikulkit (kawee@sc.chula.ac.th).
Contract grant sponsor: National Research Council of Thailand, Thailand Research Fund.

in fire. Indeed, these compounds promote dehydration and char formation.[23] However, flame retardants for cellulose textiles such as phosphoric acid are water-soluble, causing a durability problem associated with washing.[24] The immobilization of these molecules in microcapsules could help to improve the washing resistance.[25,26] In this light, the attachment of phosphodendrimers to insoluble nanoparticles could be an interesting alternative method to decrease the solubility of water-soluble phosphorus-based flame retardants, and this was the focus of this study.

In this work, the synthesis and phosphorylation of hyperbranched PAMAM polymer-grafted silica nanoparticles was attempted to immobilize the water-soluble phosphorus-based flame retardant. First, amino groups were introduced onto the silica surface by reacting the silica silanol group with the amino-functional group of the organosilane 3-aminopropyltriethoxysiliane (APTES). Next, a grafting reaction and propagation of hyperbranched PAMAM from the silica surface was achieved by reiterative two-step reaction sequences: (a) an exhaustive alkylation of primary amine (Michael addition) with methyl acrylate (MA) and (b) amidation of the amplified ester groups in the presence of a large excess of ethylenediamine (EDA) to produce primary amine terminal groups.[27] Finally, further functionalization of the terminal amino groups of hyperbranched PAMAM-grafted silica to incorporate phosphonic acid groups was carried out with conversion of the terminal amine groups into phosphonic acid groups via a Mannich type reaction. Fixation of the obtained phosphorylated hyperbranched PAMAM-grafted silica onto cotton fabric was then performed for evaluation of any resultant flame-retardant effect using a 45° flame spread rate test and thermogravimetric analysis.

EXPERIMENTAL

Materials and reagents

Fumed silica (AEROSIL 200) with a surface area of 200 m^2/g and an average particle size of 14 nm was purchased from JJ Degussa (Thailand). Methyl acrylate (MA, which was used without further purification), ethylenediamine (EDA), 3-aminopropyltriethoxysiliane (APTES) were purchased from Fluka (Switzerland). Phosphorus acid and 40% (w/v) formaldehyde were purchased from Aldrich (Germany). Toluene and methanol purchased from local supplier were distilled before use. Dialysis membrane with the molecular weight cutoff of 6000–7000 Daltons was purchased from Membrane Filtration Products (Texas). Dicyandiamide and urea as a catalyst for the phosphonic acid-functionalized silica and cellulose reaction was bought from Fluka (Switzerland). Knitted dyed industrial cotton fabric was obtained from a local textile dyeing factory.

Incorporation of amino groups onto ultrafine silica particles

The attachment of amino groups onto the silica surface was achieved by a silanization reaction between the surface silanol groups and APTES in a 600-mL flask containing 15.0 g of fumed silica into which 500 mL of 10% (v/v) toluene solution of APTES was added. The mixture was homogenously dispersed by a magnetic stirrer for 30 min. Then 50 mL of methanol : water (4 : 1 or 2 : 1) was added to the mixture and stirred for 72 h. After that, the modified silica particles were filtered and extracted with toluene for 24 h using a Soxhlet extractor to remove the unreacted APTES. The APTES-treated silica was dried in an oven at 60°C for 24 h and stored in autodehumidity desiccators [yield: 44.07% (2 : 1) and 33.44% (4 : 1)].

Grafting of hyperbranched polyamidoamine polymer on the silica surface

The Michael addition was carried out as follows: 600 mL of methanol having MA at a 10 times higher concentration than the amino content found in the treated silica was added drop by drop to 20.0 g APTES-treated silica in a 1000-mL flask, and the mixture was stirred at room temperature for 48 h. The methanol and unreacted MA were evaporated by reduced pressure evaporator, leaving PAMAM-grafted silica (product G0.5).

The amidation of the terminal ester groups from the Michael addition step was carried out as follows: The ester terminated silica (34 g) from the aforementioned Michael addition step was suspended in 500 mL of methanol in a 1000-mL round bottomed flask, and then 145 mL of 31% (v/v) EDA in methanol was added. The mixture was vigorously stirred at room temperature for 72 h. Then solvent plus some unreacted EDA was removed by a rotary evaporator at a temperature no higher than 40°C. The remaining unreacted EDA, which was hardly removed under such a mild condition, and unattached polymer products (such as hyperbranched PAMAM) were removed by dialysis. Complete removal of unwanted by-products was followed up by monitoring the pH value of the dialysate solution, leaving hyperbranched PAMAM-grafted silica (product G1.0).

These procedures were then repeated for a second (products G1.5 and G2.0, respectively) and third (products G2.5 and G3.0, respectively) round as earlier, except that a two times higher MA and EDA

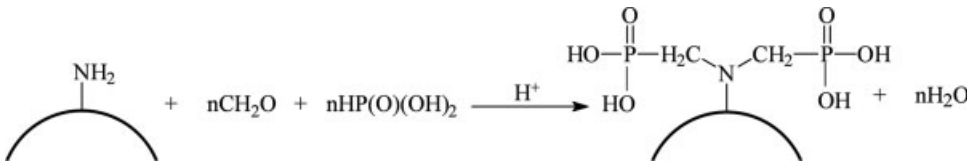

Scheme 1 The mechanism of the Mannich type reaction involving PAMAM-grafted silica, formaldehyde, and phosphorus acid.

concentration (in 100 mL of methanol) was used than that in the first round synthesis.

Phosphorylation of PAMAM-grafted silica

Hyperbranched PAMAM-grafted silica (0.2 mol amine groups), crystalline phosphorous acid (0.4 mol), and concentrated hydrochloric acid (0.6 mol) were dissolved in a total volume of 200 mL with water, and the mixture was heated to reflux in a three-necked flask fitted with thermometer, condenser, and dropping funnel. Over the course of about 1 h, 60 mL of a 40% (w/v) aqueous formaldehyde solution was added drop by drop, and the reaction was kept at the reflux temperature for an additional hour. The water was evaporated using a rotary evaporator, and the concentrate was neutralized with concentrated ammonia solution. Finally, the concentrated solution was precipitated in methanol to get a yellowish solid gel-like product. The general mechanism of this reaction (Mannich type reaction) is given in Scheme 1.

Fixation of phosphorylated hyperbranched PAMAM-grafted silica on cotton fabric

Dyed knitted cotton fabrics were treated with a solution containing 50 g/L phosphorylated hyperbranched PAMAM-grafted silica, 50 g/L urea, and 20 g/L dicyandiamide as a catalyst.[28] The application was performed using a pad mangle set to a pressure of 80% wet pick up. The padded fabric was dried at 60°C for 5 min and cured at 150°C for 3 min to allow the covalent formation of phosphonated cellulose. The treated fabric was rinsed to remove unfixed agents. To study the durability of flame retardancy, the treated cotton fabric was washed, according to TIS-121 (3-1975), in distilled water containing nonionic detergent 1 g/L at 50°C for 30 min and then rinsed the fabric with distilled water for 10 min. The fabric was dried at 60°C for 5 min and placed in a desiccator more than 24 h before conducting flammability test.

Fire retardation and thermal properties

Fire retardation of control and the treated cotton was assessed by a standard 45° flame spread test using Atlas 45° Automatic Flammability Tester according to ASTM D 1230 (in this study, the ignition time was 5 s) at 30°C and 62% ± 3% RH. The burning behavior was recorded by digital video camera. The thermal property of the treated fabric was analyzed using thermal gravimetric analysis (TGA) on a Mettler Toledo STARe System DCS822e Module.

Determination of amino group content on hyperbranched PAMAM-grafted silica

The amino group content (mmol/g of silica) of hyperbranched PAMAM-grafted silica was determined by titration. 0.1000 g of grafted silica and 25 mL of 0.01*M* hydrochloric acid aqueous solution were mixed and stirred at room temperature for 2 h, filtered and titrated with a standardized aqueous solution of 0.01*N* sodium hydroxide using phenolphthalein as an indicator.

Determination of percent grafting

The weight of hyperbranched PAMAM grafted onto the silica surface was measured by weight loss determination using TGA. The sample of hyperbranched PAMAM-grafted silica was heated to 800°C to decompose the organic content, and the percentage of grafting was calculated as relative to that of the initial silica weight as reported.[18]

Characterizations

The morphology of hyperbranched PAMAM-grafted silica was observed by scanning electron microscopy. The samples were mounted on stub with double-sided adhesive tape and coated with a thin layer of gold. Images were taken using a JEOL scanning electron microscope, JSM-5410LV, using an accelerating voltage of 15 kV, and a magnification 35,000 times of origin specimen size. The particle size distribution was analyzed using laser light scattering (Mastersizer 2000, Malvern Instruments), with a range of 0.02–2000 μm. Water/methanol mixture was employed as a dispersant. FTIR spectroscopy, taken on KBr pellet samples, was recorded on a Nicolet Fourier transform spectrophotometer (Nicolet Impact 400D). Liquid sample was cast onto KBr

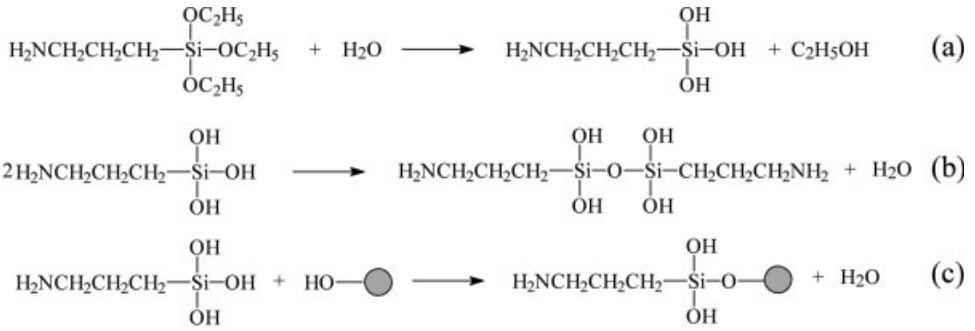

Scheme 2 Chemical equation of (a) hydrolysis reaction from alkoxysilanes, (b) self-condensation reaction, and (c) condensation reaction between APTES and silica.

plate and then solvent (methanol) was allowed to evaporate. The infrared spectrum of coated KBr plate was recorded in a range of 4000–400 cm^{-1}. The proton NMR spectra of the samples were recorded on Bruker DPX-300 spectrometer. The NMR sample tube containing a mixture of sample and solvent was placed in NMR spectrometer (DPX-300). ^1H NMR spectra were measured at the radio frequency of $\sim$ 300 MHz.

RESULTS AND DISCUSSION

Introduction of amino groups onto the silica surface

The surface functionalization of silica particles was carried out by the condensation reaction of silica silanol group with APTES, resulting in silica particles containing amino groups on the surface which acted as the initiator sites for PAMAM grafting. The condensation reaction is base-catalyzed, and APTES amine groups are a self-catalyzed component. The mechanism involved the hydrolysis of APTES triethoxy groups by water, yielding silanol groups. The subsequent condensation reaction between APTES silanol groups and silica silanol groups takes place on the silica surface as shown in Scheme 2. However, potential self-condensation of APTES can also occur and results in undesirable products. The amount of water present in the system significantly influences the hydrolysis reaction of triethoxy groups and the condensation reaction on silica surface.[29]

The rate of hydrolysis and condensation reaction was manipulated by using a methanol to water ratio of either 4 : 1 or 2 : 1. The measured amino contents (mmol/g of APTES silica) of the silica attained with different reaction times are summarized in Figure 1. The conjugated amino group content increased with an increase in both the amount of water and reaction time. Water is consumed in the conversion of APTES triethoxy groups to silanol groups (hydrolysis reaction), and hence determines the rate of hydrolysis. Consequently, the more silanol groups produced, the higher is the rate of the subsequent silanol condensation reaction. Therefore, from this data all further amino-functionalized silica for PAMAM grafting were prepared using a 2 : 1 ratio of methanol to water for 3 days.

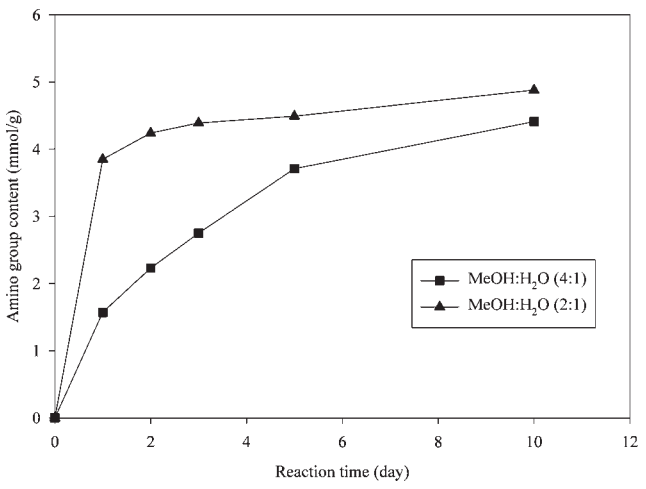

Figure 1 Amino group content of APTES-treated silica at different reaction times and methanol : water ratios.

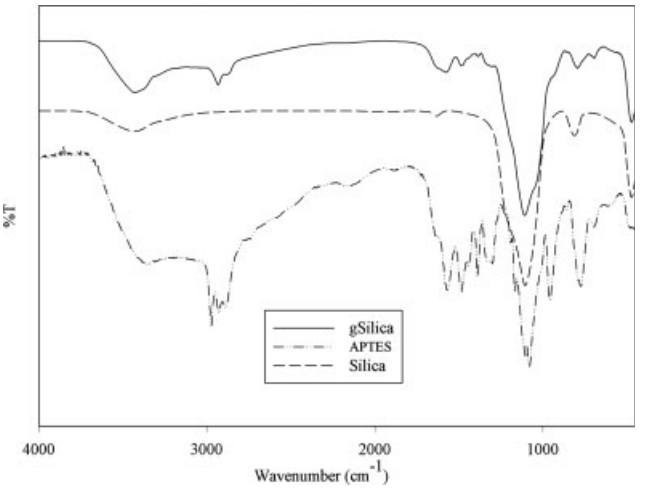

Figure 2 FTIR spectra of silica, APTES, and APTES-grafted silica (gSilica).

To confirm that APTES-functionalized silica was produced as a result of the condensation reaction, FTIR analysis was performed. Representative FTIR spectra for APTES-grafted silica, virgin silica, and APTES are shown in Figure 2. Silica, an inorganic substance, exhibited a strong absorption band of siloxane (Si—O—Si) bonding at $\sim$ 1200 cm^{-1} and the silanol OH band in the range of 3200–3400 cm^{-1}. In contrast, the putative organo-functionalized APTES-conjugated silica exhibited new absorption frequencies at 2932 and 1640 cm^{-1}, likely to be C—H stretching and primary amine (N—H) bending or (C—N) absorptions, respectively, which are absent in silica but, as expected, correspond with the absorption characteristics of the APTES spectrum which lacks the Si—O—Si and silanol OH bands. These results are consistent with APTES incorporation into the silica particles. The silica surface modification is further supported by the observed changes in spectrum pattern in the region of silanol OH band (3200–3400 cm^{-1}), because of new interhydrogen bonding interaction among APTES silica particles.

Grafting of hyperbranched PAMAM from silica surface

After the successful introduction of primary amine-functional groups to yield amino initiating sites, grafting of hyperbranched PAMAM onto the surface of amino-functionalized silica was carried out by sequentially repeating two processes, Michael addition and amidation, used in the same manner as in the synthesis of PAMAM dendrimers, for a total of three rounds of synthesis. Removal of excessive MA and EDA in each reaction step was necessary. After each Michael's addition step, excess MA was easily removed from the reaction product by reduced pressure evaporation due to its low boiling temperature. On the other hand, excess EDA from each amidation step was poorly removed by a rotary evaporation at less than 40°C and was, therefore, removed by dialysis. The purified products were subjected to FTIR analysis to monitor progress of the Michael addition and amidation reactions. Representative FTIR scans are shown in Figure 3. In the Michael addition step, the terminal methyl ester group of the products from all three successive rounds of synthesis (G0.5, G1.5, and G2.5) shows a strong and distinguishable band at 1740 cm^{-1}. This peak completely disappears from the spectra after amidation (G1.0 and G2.0) with production of the terminal amine group, corresponding to the appearance of the strong absorption intensity of the N—H band in the region of 3000–3350 cm^{-1}. Its absorption intensity significantly increases with an increase in successive synthesis rounds (and assumed PAMAM generation), reflecting that the terminal amine groups are correspondingly significantly increased. Focusing upon the final product after three rounds of synthesis (G3.0; putative hyperbranched PAMAM-grafted silica), the absorption peaks at 1649 and 1568 cm^{-1} are characteristic

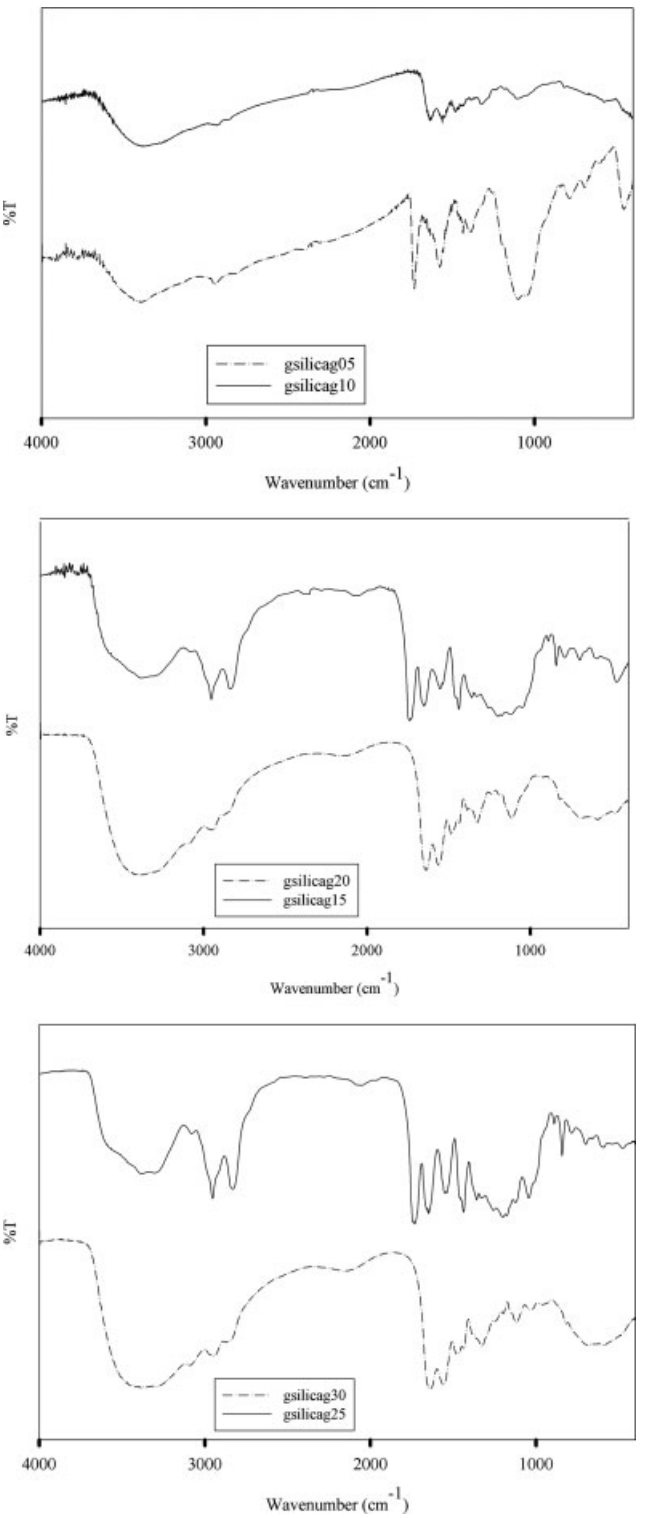

Figure 3 FTIR spectra of the products from the first, second, and third cycle synthesis (G0.5–G3.0) of hyperbranched PAMAM-grafted silicas.

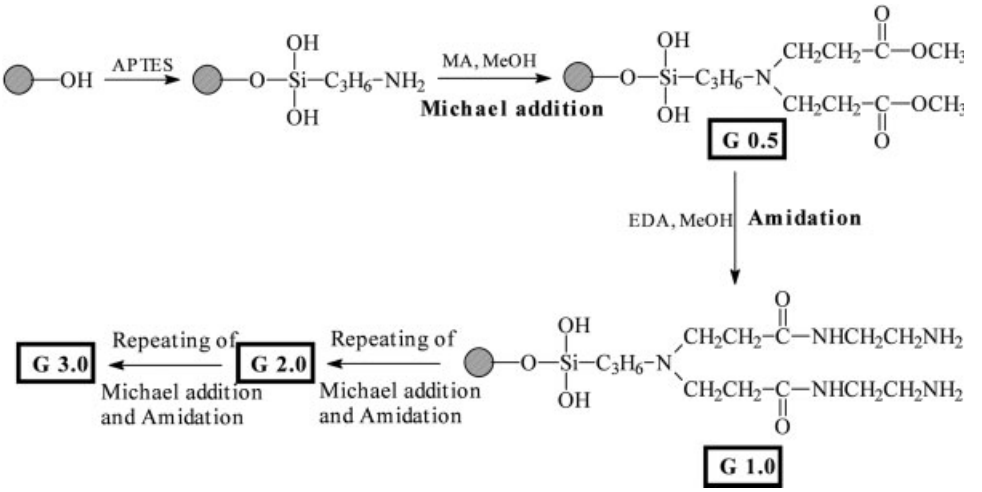

Scheme 3 The synthesis of PAMAM-grafted silica in three repeated cycles comprised sequential Michael addition and amidation reactions.

of C=O stretching and N—H bending, while those at 3281 and 3086 cm^{-1} correspond to N—H antisymmetric and symmetric stretching of primary amine, respectively. In accordance, the C—H band at 2900 cm^{-1}, which shows up strongly in the spectra of G0.5 and G1.5, becomes less dominant because of the suppressing influence of the surrounding N—H band. The expected principal reaction scheme is shown in Scheme 3.

Typical TGA thermograms of hyperbranched PAMAM-grafted silicas from the Michael and amidation reaction stages of all three reaction cycles (G0.5–G3.0) are shown in Figure 4, and reveal a clear increase in the relative thermolabile (organic) composition with increasing rounds of synthesis. To clearly quantify this, the percent graftings were calculated from these thermogram curves, and the results are summarized in Figure 5. As seen, the percent grafting with PAMAM relative to the initial silica mass increased exponentially, as was expected due to the characteristics of PAMAM dendrimer synthesis. The amino group contents, as measured after each amidation reaction, were expected to increase in line with the percent grafting. However, although a near exponential increase was observed (Fig. 5), the measured amounts are much lower than the theoretical predicted value based upon the deduced number of PAMAM moieties (Table I). Based on the reaction chemistry, there are two potential reasons why the theoretical value was not attained. First, in later stages when dense solid PAMAM branches with reduced mobility are formed, steric hindrance arising from congestion of end groups (G3 and perhaps G2) may reduce the available exposed number of sites and block the propagation of PAMAM branches. However, steric

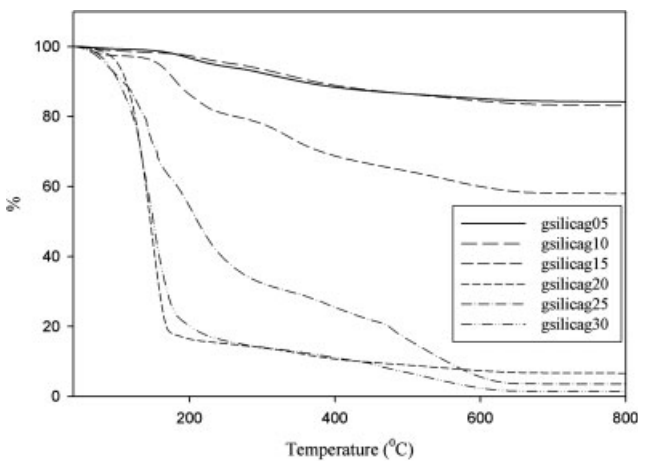

Figure 4 TGA thermograms of G0 products from the first, second and third cycle synthesis (G0.5–G3.0) of hyperbranched PAMAM-grafted silicas.

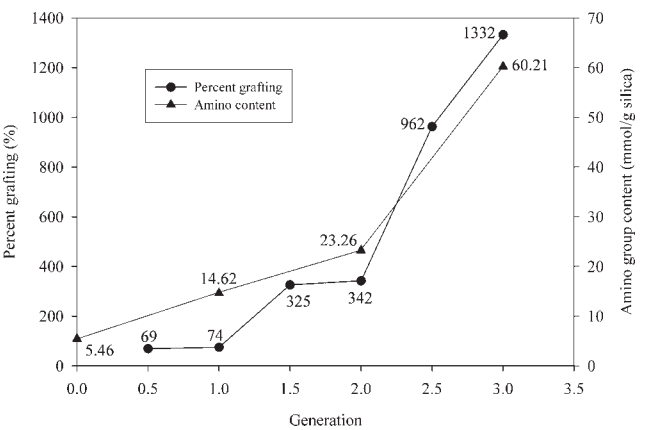

Figure 5 Percent weight grafting of PAMAM on the silica surface relative to the initial silica weight and the amino group content.

TABLE I
Amino Group Content on Silica Particle

Generation	Amino group content (mmol/g of silica)	
	Found	Theoretical
0.0	5.46	–
1.0	14.62	30.55
2.0	23.26	53.35
3.0	60.21	416.00

hindrance would not be expected to play any significant role in the earlier synthesis rounds (G1 and to some extent G2) prior to dendrimer formation. Second, the potential side reactions of one EDA with two molecules of ester groups to form intra- and inter-group cross-linked products (Scheme 4), decrease the amount of ester groups available for the next step reaction.[17]

SEM analysis and particle size analysis

Fumed silica nanoparticle powder in nature aggregated and formed micron-sized nanoclusters in suspension. Typically, physical interaction among nanoparticles is too strong to separate them back into individual particles by mechanical agitation because of their large surface area characteristics including van der Waals forces and hydrogen bonding. In this study, the effect of hyperbranched PAMAM grafting onto the silica surface was examined on particle disaggregation and its stability using SEM and particle size analysis. Typical SEM images are shown in Figure 6. As expected, the fumed silica particles as received are tightly packed and adhered together in agglomerate form. After grafting, changes in particle distribution behavior as well as the agglomerate size were observed (Fig. 6). The results indicate that hyperbranched PAMAM grafting onto silica successfully dispersed particles and reduced agglomeration, presumably because of masking of silica surface hydrogen bonding and replacement with charge repulsion (Zeta potential). In addition, as observed in the SEM images, the grafted hyperbranched PAMAM resulted in reducing the agglomerate size.

The particle size of sample was further measured with laser light scattering, and the data for fumed silica, G0.5, G1.5, and G2.5 hyperbranched PAMAM-grafted silicas are summarized in (Fig. 7). These methyl ester-terminated PAMAM-grafted particles exhibited instability in water medium. Hence, mixture of water and methanol was used as a dispersant medium. It should be noted that G1.0, G2.0, and G3.0 amine terminated hyperbranched PAMAM-grafted silicas because of their high pH value (pH $\sim$ 10) were excluded from this experiment to avoid the effect of pH on the particle size measurement. The silica particle sizes before treatment revealed a median size of $\sim$ 90 μm, while the principal population seen in the G0.5 PAMAM silica particles showed a decreased median of $\sim$ 6 μm; however, a minor population of smaller particles of 60–450 nm (median of 190 nm) was also observed. A second round of hyperbranching PAMAM synthesis (G1.5) resulted in two distinct particle size populations, with slightly more smaller ones with a reduced particle size of 40–1000 nm (median 190 nm) than larger ones with particle sizes of 1–10 μm (median 3.5 μm). Finally, the third reaction round (G2.5) resulted in a slight change in the relative proportions of small and large particles with smaller particles of a reduced sized to 50–500 nm (median 150 nm).

Phosphorylation of hyperbranched PAMAM-grafted silica

The functionalization of terminal amine groups by phosphorylation into phosphonic acid groups was

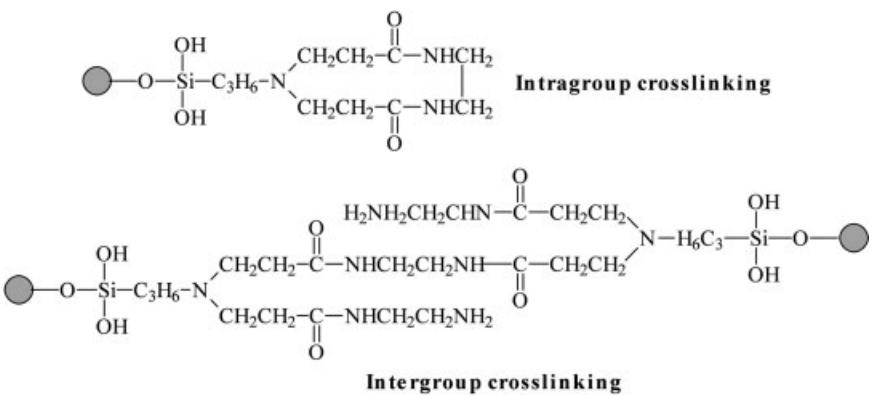

Scheme 4 Potential intra- and inter-group side reactions of the terminal amine and ester groups of hyperbranched PAMAM-grafted silica.

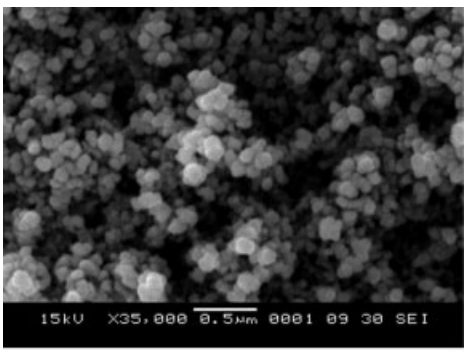

(a)

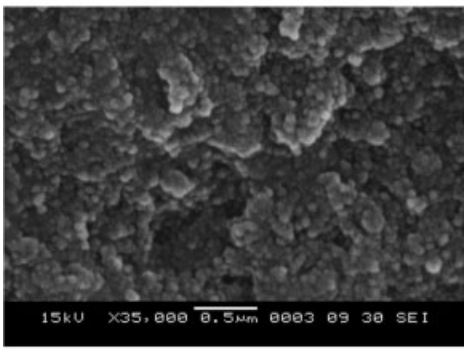

(b)

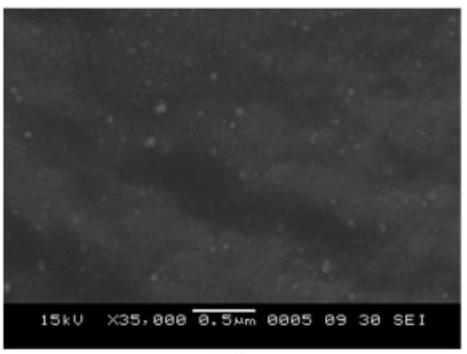

(c)

Figure 6 SEM images of (a) silica and PAMAM-grafted silica from (b) G0.5 and (c) G1.0.

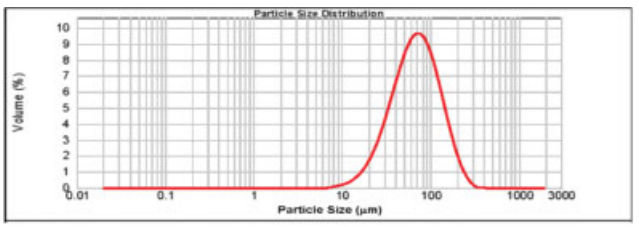

(a) Virgin silica

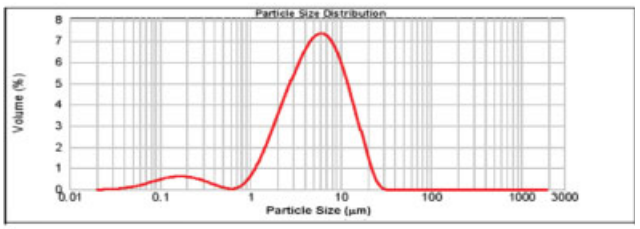

(b) gsilicag0.5

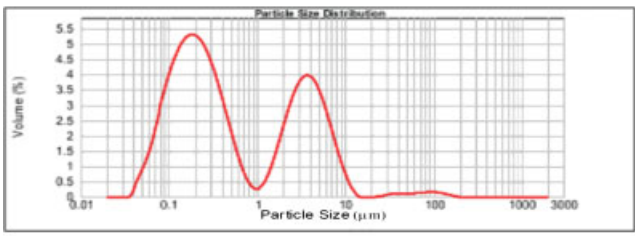

(c) gsilicag1.5

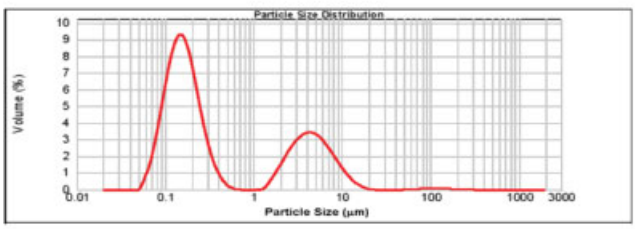

(d) gsilicag2.5

Figure 7 The particle size distribution of (a) virgin silica and PAMAM-grafted silica from (b) G0.5, (c) G1.5, and (d) G2.5. [Color figure can be viewed in the online issue, which is available at www.interscience.wiley.com.]

carried out to attempt to introduce the specific special properties of efficient chelation and flame retardancy into the hyperbranched PAMAM-grafted silica. The incorporation of phosphonic acid groups into PAMAM branch ends was easily achieved using a straightforward Mannich type reaction of phosphorous acid with formaldehyde and primary amine compounds at low pH in the presence of ~ 2–3 mol of concentrated hydrochloric acid per mole of an amine (Scheme 5 and Fig. 8).

The reaction products were characterized using FTIR (Fig. 9). Considering the spectrum of phosphonic acid-functionalized silica, new peaks are observed, indicating a change in the structure of hyperbranched PAMAM-grafted silica. The presence of the phosphonic acid moiety corresponds to the absorption bands at 1182, 1078, and 923 cm^{-1} for (P═O), (P─OH), and (P─O) groups, respectively.[30–33] The very broad band extending from 3600 cm^{-1} to as low as 2500 cm^{-1} is likely to be due to the absorption characteristic of the phosphonic acid hydroxyl group (OH). The N─H stretching band at 3500 cm^{-1} in

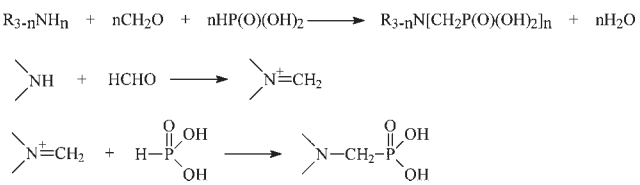

Scheme 5 The Mannich reaction involving an amine, formaldehyde, and phosphorous acid.

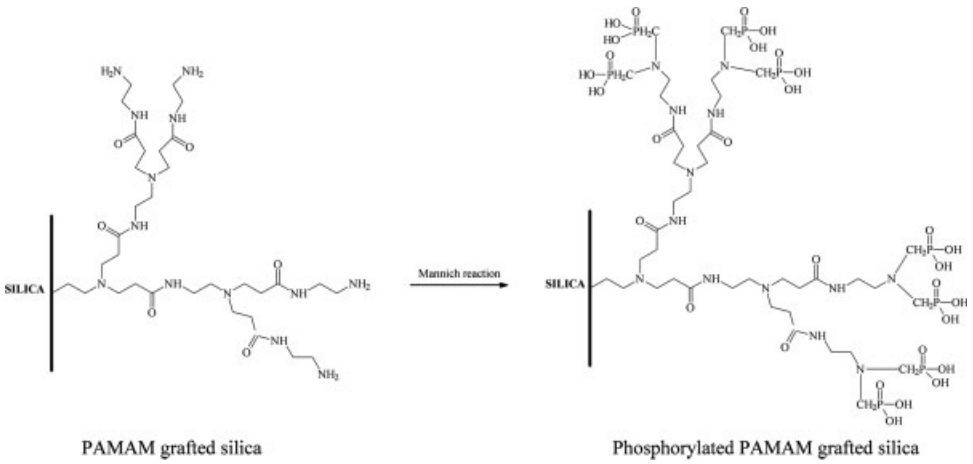

Figure 8 The putative structure of phosphonic acid-functionalized PAMAM-grafted silicas.

hyperbranched PAMAM-grafted silica markedly decreased, reflecting its conversion by the Mannich reaction. In agreement, the ^{1}H NMR spectrum of phosphonic acid-functionalized PAMAM-grafted silica (Fig. 10) indicated the presence of C(1)-H_2 and C(2)-H_2 groups (3.6 ppm) and a methylene group adjacent to phosphorous nucleus (3.7 ppm). Thus, FTIR and ^{1}H NMR results both provide strongly supporting evidence that phosphonic acid groups successfully replaced hyperbranched PAMAM-grafted silica amine groups, leading to hyperbranched polymer-grafted silica.

Flame retardancy effect testing

Phosphorylated hyperbranched PAMAM-grafted silica potentially offers both strong chelating powers and flame retardancy properties. The latter was tentatively investigated in this study. Preliminary evaluation of flame retardancy effect on cotton fabric was undertaken. Cotton substrate was chosen because of its relatively high flammability characteristic as well as common usage. In a standard 45° burning test, phosphorylated hyperbranched PAMAM-grafted silica-treated cotton exhibits a marked fire retardancy property as shown in Figure 11. The burning test shows no ignition after flaming for the unwashed treated fabric. In case of the untreated control, fabric is ignited easily and burned severely. The flame spreads very quickly and burns the entire fabric. After washing, the treated fabric is still able to exhibit satisfactory flame retardancy performance, indicating the durable property of phosphorylated hyperbranched PAMAM-grafted silica. A large amount of char and molten viscous layer are formed on the fabric's surface, acting as an insulation layer, and then protecting fabric from flame and oxygen to further decompose the fabric.

In addition, analysis of treated and untreated cotton fabric was performed by TGA analysis, with representative thermograms shown in Figure 12. The untreated fabric starts to decompose at about 300°C and rapidly increases from 330°C reaching 100% weight loss at 350°C, as reported earlier.[34] Degradation of the treated fabric begins at the relatively lower temperature of 260°C and progresses rapidly from 300°C, leaving about 35% residual weight (at 320°C). Thereafter, a slow decomposition to about 2–3% residual weight by $\sim$ 600°C due to the retardant effect of phosphonate silica was observed. The pyrolysis of the flame-retardant-treated cotton fabric typically starts at a relatively lower decomposition temperature because of the catalytic dehydration of cellulose by the flame retardant, leading to char formation on the fabric surface, a well-established flame retardantcy mechanism of phosphorus-containing compounds. In this scenario, the decline of

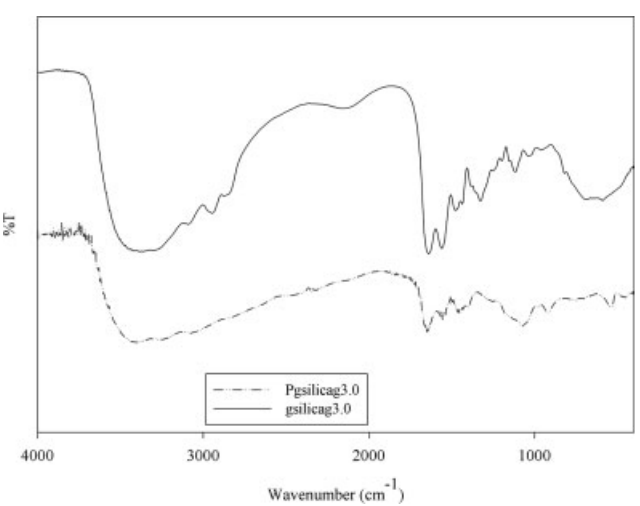

Figure 9 FTIR spectra of G3.0 hyperbranched PAMAM-grafted silica (gsilica 3.0) and its phosphorylated derivative (Pgsilica 3.0).

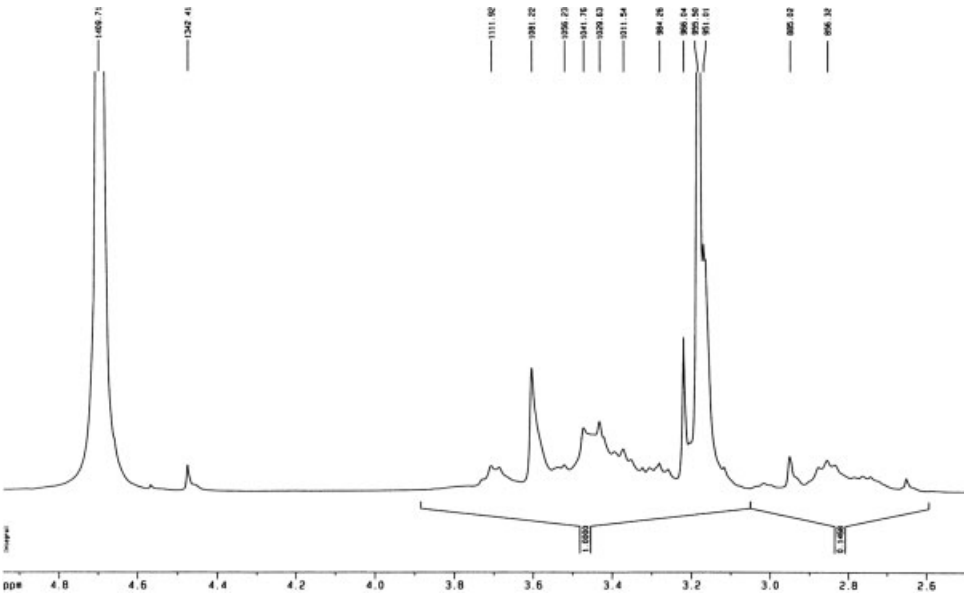

Figure 10 ^{1}H NMR spectrum of phosphorylated hyperbranched PAMAM-grafted silica.

degradation temperature is due to the reaction of the phosphonic acid with the C_6 hydroxyl of the cellulose anhydroglucose unit, blocking the formation of levoglucosan (source of fuel) and so promoting char rather than flame formation. As a result, the percentage weight loss for treated fabric measured at 350°C (the temperature of 100% weight loss of untreated fabric) is reduced to 70%, supporting the flame-retardant effect of phosphorylated hyperbranched PAMAM-grafted silica. Moreover, PAMAM contains nitrogen atoms that act synergistically with phosphorus[35] enhancing the electrophilicity of phosphorous and, through making a stronger Lewis acid, promoting the phosphorylation reaction with C-6 hydroxyl group of anhydroglucose unit. TGA thermogram of treated fabric after washing presented in Figure 12 shows the decomposition temperature at 280°C, which is higher than those of unwashed fabric but lower than that of control fabric. This result indicates that the phosphoester linkages between the phosphorylated PAMAM-silica and C-6 hydroxyl groups exhibit wash-off resistance.

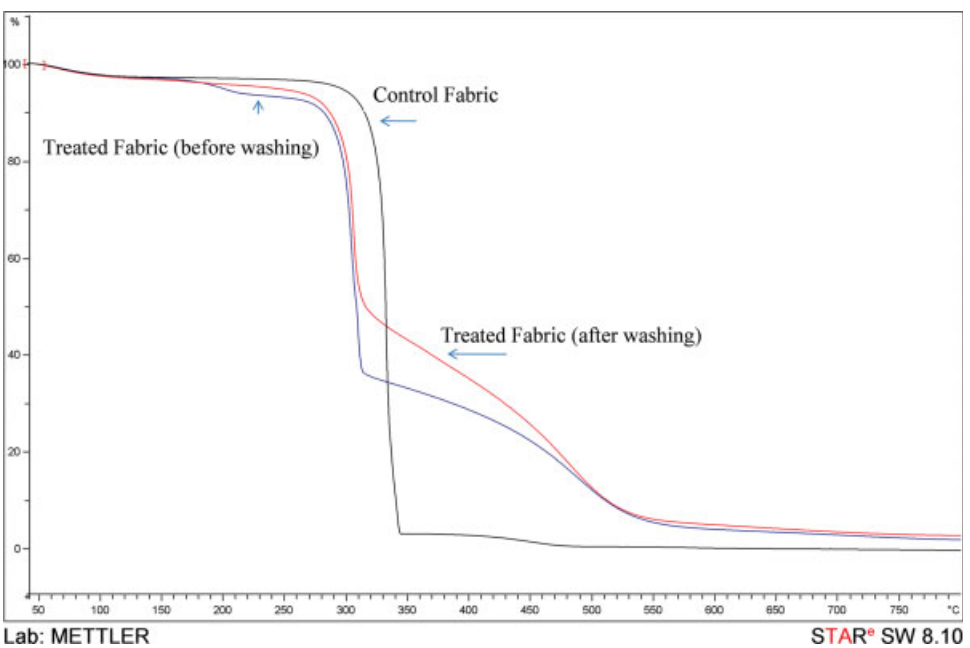

Figure 11 TGA thermograms of untreated cotton fabric and treated cotton fabrics (before and after washing). [Color figure can be viewed in the online issue, which is available at www.interscience.wiley.com.]

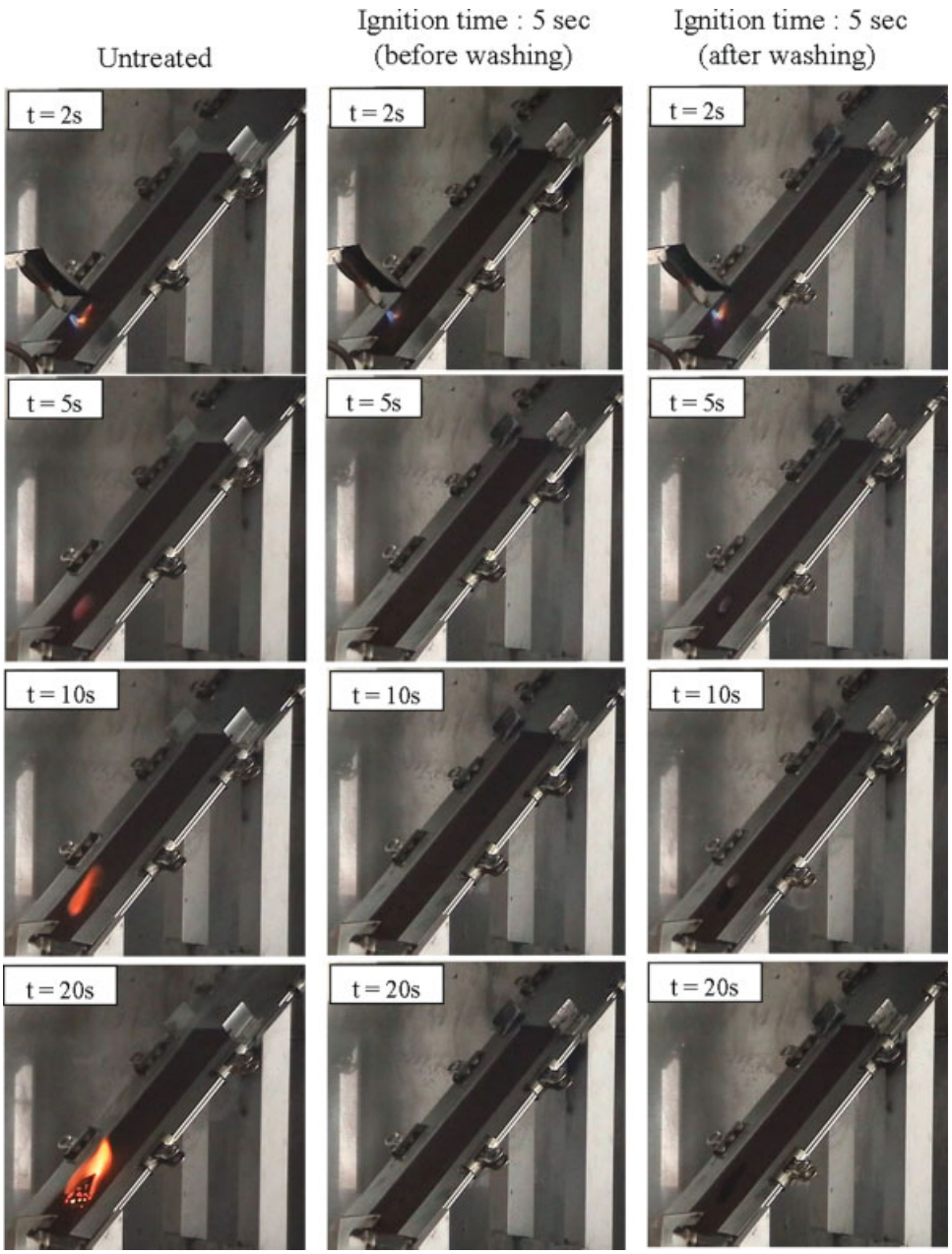

Figure 12 Flame spread test of untreated cotton fabric and treated cotton fabrics (before and after washing). [Color figure can be viewed in the online issue, which is available at www.interscience.wiley.com.]

From this finding, it is reasonable to say that an immobilization of the water-soluble compound (phosphodendrimers to insoluble nanoparticles) could help improve its durability to washing.

CONCLUSIONS

The grafting of hyperbranched PAMAM polymer onto amino group-functionalized silica was successfully achieved by performing three rounds of paired reactions comprised a Michael addition of the silica amino group to methyl acrylate and the amidation of the resulting terminal methyl ester group with ethylenediamine. The percent grafting, relative to the initial silica weight and calculated from TGA results, were 74, 342, and 1332% for the three reaction cycles, respectively, with corresponding amino group contents of 14.6, 23.3, and 60.2 mmol/g silica, respectively. However, the attained amino group contents were much lower than the expected values relative to the amount of grafting, perhaps due to the effect of steric hindrance in later cycles as hyperbranched PAMAM are formed, and the intra- and inter group crosslinking. Regardless, grafted hyperbranched PAMAM enhanced particle dispersion and reduced particle agglomeration. Thus, the

agglomerate particle size before grafting averaged $\sim$ 70 μm and after grafting the particle size significantly decreased to a range of 50–500 nm (average $\sim$ 150 nm) with major composition of the two discrete populations.

The phosphorylation of the hyperbranched PAMAM polymer terminal amino groups was also successfully achieved by the Mannich type reaction. The phosphorylated products containing the phosphonic acids exhibited flame retardancy when applied onto flammable cotton fabric. After washing test, the hyperbranched PAMAM polymer showed good retention of fire retardancy, indicating its wash-off resistancy performance.

References

1. Tomalia, D. A. Prog Polym Sci 2005, 30, 294.
2. Lee, C. C.; Mackay, J. A.; Frechet, J. M. J.; Szoka, F. C. Nat Biotechnol 2005, 23, 1517.
3. Tomalia, D. A.; Baker, H.; Dewald, J.; Hall, M.; Kallos, G.; Martin, S. Polym J (Tokyo) 1985, 17, 117.
4. Aulenta, F.; Hayes, W.; Rannard, S. Eur Polym J 2003, 39, 1741.
5. Smith, D. K.; Hirst, A. R.; Love, C. S.; Hardy, J. G.; Brignell, S. V.; Huang, B. Q. Prog Polym Sci 2005, 30, 220.
6. Pan, B.; Gao, F.; Ao, L.; Tian, H.; He, R. D.; Cui, D. Colloid Surf A 2005, 259, 89.
7. Gong, A. J.; Chen, Y. M.; Zhang, X.; Liu, H. W.; Chen, C. F.; Xi, F. J Appl Polym Sci 2000, 78, 2186.
8. Demadis, K. D.; Neofotiston, E. Chem Mater 2000, 19, 581.
9. Shi, X.; Lesniak, W.; Islam, M. T.; Muñiz, M. C.; Balogh, L. P.; Baker, J. R. Colloid Surf A 2006, 272, 139.
10. Ahmed, S. M.; Budd, D. M.; McKeown, N. B.; Evans, K. P.; Beaumont, G. L.; Donaldson, C.; Brennan, C. M. Polymer 2001, 42, 889.
11. Majoros, I. J.; Keszler, B.; Woehler, S.; Bull, T.; Baker, J. R. Macromolecules 2003, 36, 5526.
12. Heldt, J. M.; Durand, N. F.; Salmain, M.; Vessiè, A.; Jaouen, G. J Organomet Chem 2004, 689, 4775.
13. Yoshimaru, T.; Abe, S.; Esumi, K. Colloid Surf A 2004, 251, 141.
14. Li, H. Y.; Chen, H. Z.; Xu, W. J.; Yuan, F.; Wang, J. R.; Wang, M. Colloid Surf A 2005, 254, 173.
15. Bergemann, K.; Fanghänel, E.; Knackfuβ, B.; Lüthge, T.; Schukat, G. Carbon 2004, 42, 2338.
16. Park, S. J.; Seo, M. K.; Nah, C. J Colloid Interface Sci 2005, 291, 229.
17. Qu, R.; Niu, Y.; Sun, C.; Ji, C.; Wang, C.; Cheng, G. Microporous Mesoporous Mater 2006, 97, 58.
18. Tsubokawa, N.; Ichioka, H.; Satoh, T.; Hayashi, S.; Fujiki, K. React Funct Polym 2008, 37, 75.
19. Wu, X. Z.; Liu, P.; Pu, Q. S.; Sun, Q. Y.; Su, Z. X. Talanta 2004, 62, 918.
20. Taniguchi, Y.; Shirai, K.; Saitoh, H.; Yamauchi, T.; Tsubokawa, N. Polymer 2005, 46, 2541.
21. Jiang, Y.; Gao, Q.; Yu, H.; Chen, Y.; Deng, F. Microporous Mesoporous Mater 2007, 103, 316.
22. Perignon, N.; Marty, J. D.; Mingotaud, A. F.; Dumont, M.; Rico-Lattes, I.; Mingotaud, C. Macromolecules 2007, 40, 3034.
23. Horrocks, A. R. Polym Degrad Stab 1996, 54, 143.
24. Charuchinda, S.; Srikulkit, K.; Mowattana, T. J Sci Res Chula Univ 2005, 30, 98.
25. Giraud, S.; Bourbigot, S.; Rochery, M.; Vroman, I.; Tighzert, L.; Delobel, R. Polym Degrad Stab 2002, 77, 285.
26. Giraud, S.; Bourbigot, S.; Rochery, M.; Vroman, I.; Tighzert, L.; Delobel, R.; Pouth, F. Polym Degrad Stab 2005, 88, 106.
27. Esfand, R.; Tomalia, D. A. In Dendrimers and Other Dendritic Polymers; Fréchet, J. M. J.; Tomalia, D. A., Eds.; Wiley: Chichester, 2001; p 587.
28. Gillingham, E. L.; Lewis, D. M.; Srikulkit, K. Color Technol 2001, 107, 318.
29. Simon, A.; Cohen-Bouhacina, T.; Porté, M. C.; Aimé, J. P.; Baquey, C. J Colloid Interface Sci 2002, 251, 278.
30. Demadis, K. D.; Katarachia, S. D. Phosphorus, Sulfur Silicon Relat Elem 2004, 179, 627.
31. Heras, A.; Rodriguez, N. M.; Ramos, V. M.; AgullÓ, E. Carbohydr Polym 2001, 44, 1.
32. Chaplais, G.; Bideau, J. L.; Leclercq, D.; Vioux, A. Chem Mater 2003, 15, 1950.
33. Danilich, M. J.; Burton, D. J.; Marchant, R. E. Vib Spectrosc 1995, 9, 229.
34. Zhu, P.; Sui, S.; Wang, B.; Sun, K.; Sun, G. J Anal Appl Pyrolysis 2004, 71, 645.
35. Gaan, S.; Sun, G. J Anal Appl Pyrolysis 2007, 78, 371.